doi:10.3772/j.issn.1006-6748.2021.02.010

Joint position control of bionic jumping leg driven by pneumatic artificial muscle①

Su Hongsheng (苏红升), Ding Wei, Lei Jingtao②
(School of Mechatronic Engineering and Automation, Shanghai University, Shanghai 200072, P. R. China)

Abstract

The bionic legs are generally driven by motors which have the disadvantages of large size and heavy weight. In contrast, the bionic legs driven by pneumatic artificial muscles (PAMs) have the advantages of light weight, good bionics and flexibility. A kind of bionic leg driven by PAMs is designed. The proportional-integral-derivative (PID) algorithm and radial basis function neural network (RBFNN) algorithm are combined to design RBFNN-PID controller, and a low-pass filter is added to the control system, which can effectively improve the jitter phenomenon of the joint during the experiment. It is verified by simulation that the RBFNN-PID algorithm is better than traditional PID algorithm, the response time of joint is improved from 0.15 s to 0.07 s, and the precision of joint position control is improved from 0.75 ° to 0.001 °. The experimental results show that the amplitude of the change in error is reduced from 0.5 ° to 0.2 °. It is verified by jumping experiment that the mechanism can realize jumping action under control, and can achieve the horizontal displacement of 500 mm and the vertical displacement of 250 mm.

Key words: pneumatic artificial muscle (PAM), bionic leg, radial basis neural network, position control

0 Introduction

With the advancement of science and technology, bionic robots are widely used in various occasions. Robots that study biological motion mechanisms mainly include wheeled mobile robots, walking robots, snake-shaped robots, crawler mobile robots, crawling robots[1], etc. However, in practical applications such as archaeological exploration, interstellar exploration, military reconnaissance, and counter-terrorism activities, the terrain environment is usually very complex. Wheeled and tracked robots can only work on flat ground, and once the terrain is uneven, its movement is greatly restricted. The walking or crawling robots are characterized by many degrees of freedom, complex control and slow movement, so they are unable to work in large obstacles or ditches. In contrast, bionic robots have good bionics and can adapt to various complex terrain environments.

The single-legged robot, which has the characteristics of simple structure, insufficient drive and poor balance, has only one-step jumping state. Its research is helpful to explore the nature of jumping and it is an ideal platform to study the jumping principle and control strategy of jumping robot[2]. Observing animals' jumping process shows that when the instantaneous speed of the leg reaches a certain value, it leaves the ground and moves upward, thus achieving the jumping action[3]. In the researches of jumping robots, researchers usually adopt the motor power as driving force for jumping. The disadvantages of bionic legs driven by motors are its large weight and bad bionics. In contrast, bionic legs driven by pneumatic artificial muscles (PAMs) have the advantages of light weight, good bionics and flexibility. Due to its inherent strong nonlinearity and time lag, PAMs are difficult to achieve high precision control[4].

Scholars have carried out some researches about joint position control of bionic legs driven by one PAM. Ref. [5] used feedforward control algorithm and nonlinear proportional integral (PI) control algorithm to improve the response speed and the precision of joint position control. The precision of joint position control reached ±0.2 °, and the steady-state precision of the joint reached ±0.1 °. Refs[6-10] used sliding mode variable structure to control joints. Experiments showed that the precision of sliding mode variable structure control (SMC) algorithm was higher than the tradition-

① Supported by the National Natural Science Foundation of China (No. 51775323).
② To whom correspondence should be addressed. E-mail: jtlei2000@163.com
Received on Apr. 30, 2020

al proportional-integral-derivative (PID) algorithm. Ref. [11] proposed a cascade control strategy based on a robust modeling method. Under the experimental conditions where the upper limit of the operating frequency was less than 1.25 rad/s, the joint achieved a steady-state tracking of the reference trajectory of less than 2%. Ref. [12] used a nonlinear PID controller to control the joint position, and the results showed that the nonlinear PID controller had good dynamic performance and robustness. Ref. [13] adopted position error, position error rate and load change as internal feedback loop to control the robot, thus improved the characteristic of time lag of PAMs. Ref. [14] proposed a controller that combined neuron PI algorithm and feedforward control algorithm for joint position control of rehabilitation robots. Refs[15-19] combined fuzzy control algorithm with PID control algorithm. The simulation results showed that the fuzzy PID control algorithm had the characteristics of small overshoot, fast response time and strong robustness, and can effectively improved the comprehensive control effect of the system. Ref. [20] used neural network compensation PID control algorithm to control the joint position and stiffness of the bionic quadruped robot. Simulation results showed that the joint position can be controlled well under the condition of given joint stiffness. In these joint position control schemes, the controlled objects are mostly robotic arms and rehabilitation robot joints. Few scholars study joints for jumping. Some scholars use fuzzy PID to control joints for jumping, but the joint position curve for simulation is a sine curve. This is inconsistent with the variation rule of the actual joint position for jumping, and there is no experimental verification. Different from general rehabilitation robot joint control, the requirements about the response speed and control stability of joint for jumping action are high.

A bionic leg driven by one PAM is presented, and the expected change curve of joint position for jumping is obtained. A method based on non-model radial basis function neural network (RBFNN) combined with PID controller is proposed to improve the strong nonlinearity of PAMs. In the experiment, the intelligent control algorithm can cause the problem of joint jitter in the control process. To solve this problem, a filter is added to the control loop to optimize the controller.

1 Bionic leg modeling

1.1 Bionic leg

A single-degree-of-freedom bionic leg is designed with the ankle joint of kangaroo as the bionic object, as shown in Fig. 1. The leg is driven by one PAM and one spring.

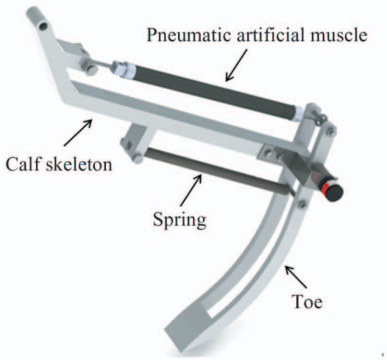

Fig. 1 Bionic jumping leg

The PAM is DMSP-10-300N-RM-RM type produced by FESTO company, which has a maximum contraction rate of 25%. Thus the rotation angle of the joint can reach 80 °.

1.2 Mathematical model of joint control system

1.2.1 Force model of PAM

In the researches of force model of PAM, the model of Ref. [21] based on the principle of conservation of energy and the principle of virtual work is currently commonly used:

$$\begin{cases} \boldsymbol{F} = p[a(1-\varepsilon^2)-b] \\ b = \dfrac{\pi D_0^2}{4\sin^2\alpha_0} \\ \varepsilon = \dfrac{\Delta l}{l} \\ a = \dfrac{\pi D_0^2}{4} \end{cases} \tag{1}$$

where, $\boldsymbol{F}$, p and ε are the contractile force, inflation pressure, and contraction rate of PAM; D_0 and α_0 are the initial diameter and initial knitting angle of PAM; Δl and l are the contracted length and initial length of PAM.

1.2.2 Kinematics

Schematic diagram of the bionic leg structure is shown in Fig. 2.

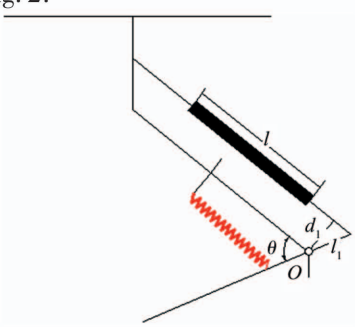

Fig. 2 Schematic diagram of bionic leg structure

According to the mathematical geometric relationship of the bionic leg, the formulas of joint kinematics model can be obtained as

$$\varepsilon = (\cos\theta_0 - \cos\theta) \cdot l_1 / l \tag{2}$$

$$d_1 = l_1 \sin\theta \tag{3}$$

where θ_0 is the initial position of the joint, θ is the current position of the joint, l_1 is the distance from the connector of PAM to the joint rotation center O, and d_1 is the vertical distance between the PAM and the joint rotation center O.

1.2.3 Dynamics

The mass of the toe is 0.27 kg, which is negligible compared with the 1.7 kg of the calf skeleton. Therefore, the joint torque is provided by the force of PAM and the force of spring. Joint torque can be expressed as

$$\boldsymbol{\tau} = \boldsymbol{F} d_1 - k_s \cdot \Delta\delta \tag{4}$$

where $\boldsymbol{\tau}$ is joint torque, k_s is the stiffness of spring, and $\Delta\delta$ is the variation of joint position.

The formulas for deriving joint torque based on Lagrange dynamics are[22]

$$\boldsymbol{\tau} = \frac{\mathrm{d}}{\mathrm{d}t}\left(\frac{\partial L}{\partial \dot{\boldsymbol{\theta}}}\right) - \frac{\partial L}{\partial \boldsymbol{\theta}} \tag{5}$$

$$\boldsymbol{\tau} = \frac{\mathrm{d}}{\mathrm{d}t}\left(\frac{\partial E_k}{\partial \dot{\boldsymbol{\theta}}}\right) - \frac{\partial E_k}{\partial \boldsymbol{\theta}} + \frac{\partial E_p}{\partial \boldsymbol{\theta}} \tag{6}$$

where, L is the Lagrange function of system, E_k is the kinetic energy of system, E_p is the potential energy of system, and t is time. The joint torque can be obtained by calculating the kinetic energy and potential energy of the system in turn and substituting them into the above equation.

$$\boldsymbol{\tau} = A - B \tag{7}$$

$$A = \left[\left(\frac{1}{4} m_1 l_1^2 + J_1\right) + m_2 l_1^2\right] \ddot{\boldsymbol{\theta}} \tag{8}$$

$$B = \left(\frac{1}{2} m_1 g l_1 + m_2 g l_1\right) \cos\left(\frac{\pi}{4} - \theta\right) \tag{9}$$

where, m_1 is the mass of the toe, J_1 is the moment of inertia from the center of mass of the toe to the center of rotation, and m_2 is the mass of the calf skeleton.

2 RBFNN-PID control algorithm

PAMs have strong nonlinearity and hysteresis. By taking advantage of the characteristics of radial basis function (RBF) network, the conventional PID controller can be adjusted to achieve better control effect when controlling nonlinear objects.

Fig. 3 shows the RBFNN-PID control system, which consists of a PID controller, RBF neural network, and the controlled object. Among them, $r(k)$ and $y(k)$ are the input and output of the control system, $e(k)$ and $u(k)$ are the input and output of the PID controller, and $y_m(k)$ is the identification output of the RBF neural network. ΔK_p, ΔK_i, ΔK_D are the adjustments of the PID controller parameters.

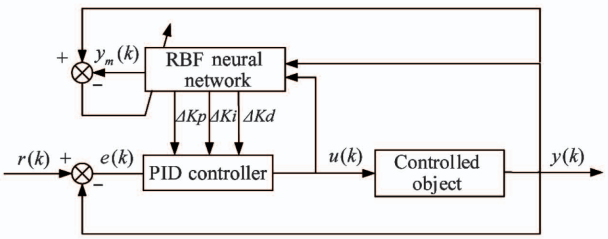

Fig. 3 RBFNN-PID control system

Set the theoretical output of the identification system at time k be $y(k)$ and the output of the identification network be $y_m(k)$, and set the performance index function of the identifier as

$$E_i = \frac{1}{2}[y(k) - y_m(k)]^2 \tag{10}$$

According to the gradient descent method, the iterative algorithm of center node, node base width parameters and output weight can be obtained as follows.

Center node:

$$\Delta c_{ji} = [(y_{out}(k) - y_m(k))] w_j \frac{x_i - c_{ji}}{b_j^2} \tag{11}$$

$$c_{ji}(k) = c_{ji}(k-1) + C \tag{12}$$

$$C = \eta \Delta c_{ji} + \alpha[c_{ji}(k-1) - c_{ji}(k-2)] \tag{13}$$

Base width parameters:

$$\Delta b_j = [(y_{out}(k) - y_m(k))] w_j h_j \frac{\| \boldsymbol{X} - \boldsymbol{C}_j \|^2}{b_j^3} \tag{14}$$

$$b_j(k) = b_j(k-1) + D \tag{15}$$

$$D = \eta \Delta b_j + \alpha[b_j(k-1) - b_j(k-2)] \tag{16}$$

Output weight:

$$W_j(k) = \eta[y_{out}(k) - y_m(k)] h_j + E \tag{17}$$

$$E = w_j(k-1) + \alpha[w_j(k-1) - w_j(k-2)] \tag{18}$$

where α and β are the momentum factor and the learning rate, respectively.

The sensitivity information of the output of the object to the control input is the Jacobian matrix algorithm:

$$\frac{\partial y_{out}}{\partial u} = \frac{\partial \sum_{j=1}^{m} w_j h_j}{\partial u} = \sum_{j=1}^{m} w_j h_j \left[\frac{(c_j - x_1)}{2 b_j^2}\right] \tag{19}$$

Set the neural network setting index be

$$E(k) = \frac{1}{2}[r(k) - y(k)]^2 = \frac{1}{2} e(k)^2 \tag{20}$$

The three inputs of PID are

$$\begin{cases} xc(1) = e(k) - e(k-1) \\ xc(2) = e(k) \\ xc(3) = e(k) - 2e(k-1) + e(k-2) \end{cases} \tag{21}$$

The incremental PID algorithm is

$$u(k) = u(k-1) + \Delta u(k) \tag{22}$$

$$\Delta u(k) = k_p xc(1) + k_i xc(2) + k_d xc(3) \tag{23}$$

The adjustment algorithms of k_p, k_i, k_d can be obtained from the gradient descent method and Jacobi information of the controlled object:

$$\begin{cases} \Delta k_p = \eta e(k) \dfrac{\partial y}{\partial u} xc(1) \\ \Delta k_i = \eta e(k) \dfrac{\partial y}{\partial u} xc(2) \\ \Delta k_d = \eta e(k) \dfrac{\partial y}{\partial u} xc(3) \end{cases} \tag{24}$$

3 Simulation

3.1 Expected joint angle position

The bionic leg centroid requires a certain initial velocity at the moment of leaving the ground, which can ensure the bionic leg hop smoothly and cross an obstacle of a certain height. It is necessary to plan the centroid motion of the bionic leg.

Variable quintic polynomial is used to compare with the centroid motion of the bionic leg. The centroid trajectory of leg during the take-off stage is planned as

$$\begin{cases} x(t) = \sum_{i=0}^{5} a_i t^i + u_1 (t - t_s)^{\lambda_1} (t - t_f)^{\lambda_2} \\ y(t) = \sum_{i=0}^{5} b_i t^i + u_2 (t - t_s)^{\lambda_3} (t - t_f)^{\lambda_4} \end{cases} \tag{25}$$

where $x(t)$ and $y(t)$ are the coordinates of the bionic leg centroid in the x-direction and y-direction of the foot-end coordinate system at the time of t; a_i, $b_i (i = 1, 2, 3, 4, 5)$ are polynomial coefficients; u_1, u_2, λ_j $(j = 1, 2, 3, 4, \lambda_j \geqslant 3)$ are curve tunable parameters; t_s, t_f are the initial and end time of the jump phase respectively.

The motion space of the center of mass in the reference coordinate system is calculated, the motion constraint of the center of mass is introduced into the variable fifth-order polynomial, and the value of adjustable parameters is adjusted to make the center of mass fall within the motion space. The trajectory equation is incorporated into the inverse kinematics solution to obtain the change function of joint position and time, as shown in Fig. 4. The time of jumping is 0.4 s and the rotatory joint varies from 66 ° to 97 °.

3.2 Simulation results

The simulation block diagram is established by combining the controller and the mathematical model of the joint control system. Set the initial parameters of the PID of the two controllers to be the same, and use the jump joint position curve planned above as the expected signal curve. Run the simulation to get the trajectory tracking curve 1 and trajectory tracking error curve 1 as shown in Fig. 4 and Fig. 5. The results of neural network identification are shown in Fig. 6.

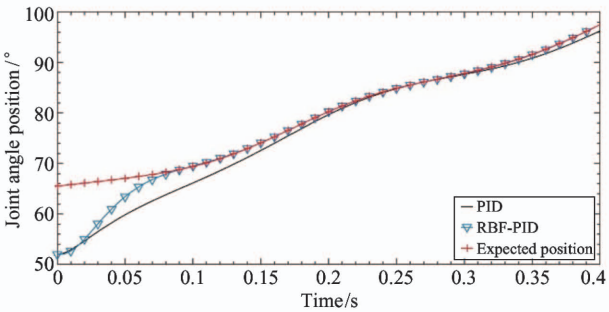

Fig. 4 Trajectory tracking curve 1

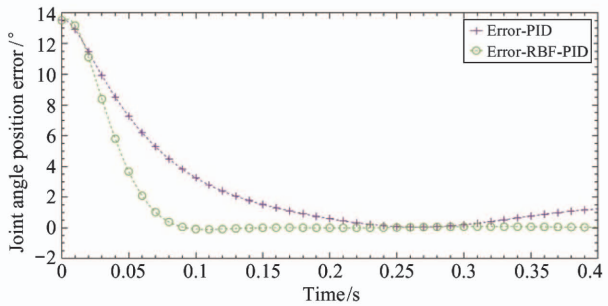

Fig. 5 Trajectory tracking error curve 1

As shown in Fig. 4 and Fig. 5, the effect of RBFNN-PID control algorithm is obviously better than traditional PID control algorithm. Firstly, the RBFNN-PID control algorithm has faster response time, which is 0.15 s less than PID control algorithm, and the error is close to 0 at the time of 0.09 s. Secondly, the RBFNN-PID control algorithm has no overshoot, and reaches the steady state at the time of 0.1 s. The steady-state error of traditional PID reaches 1.25 ° −1.5 °.

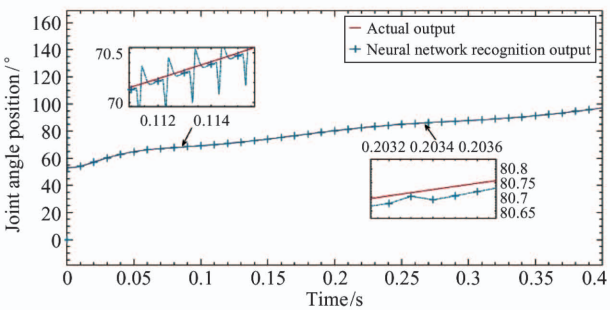

Fig. 6 Neural network identification results

It can be seen from Fig. 6 that the identification output of the RBFNN is basically the same as actual

output, and the maximum error is only about 0.5 °.

4 Experiment

4.1 Experiment platform

In order to verify the proposed control algorithm, the bionic jumping experiment is conducted with the Simulink real-time control software platform.

The experimental system includes bionic leg, ITV0050 electric proportional valve of SMC company, WDH22L non-contact angle sensor of SENTOP company, NI multifunctional data acquisition card, as shown in Fig. 7.

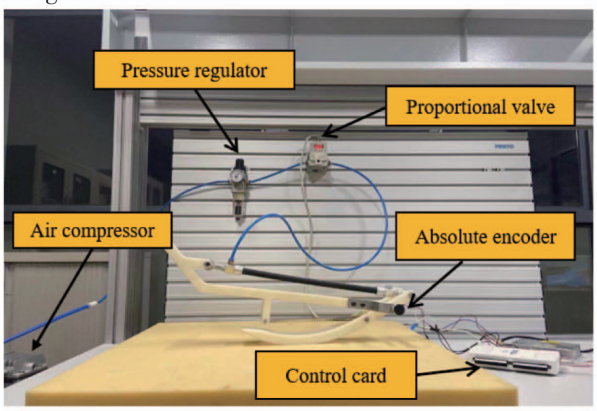

Fig. 7 Experiment platform

4.2 Joint position control experiment

The trajectory of the joint position curve and error curve are obtained through experiments, as shown in Fig. 8 and Fig. 9.

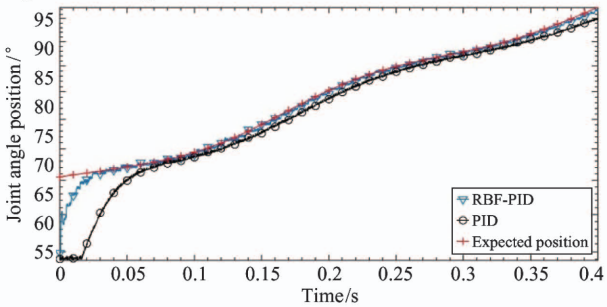

Fig. 8 Trajectory tracking curve 2

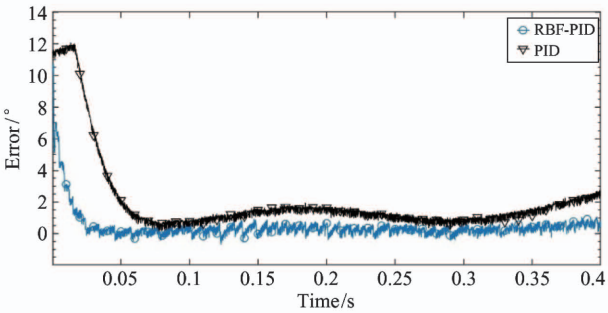

Fig. 9 Trajectory tracking error curve 2

The experimental results show the superiority of RBFNN-PID control algorithm. Compared with PID control algorithm, RBFNN-PID control algorithm has fast response time. At the time of 0.03 s, the trajectory error of the joint position is decreased to about 0.5 ° and the joint following error is maintained within 1 ° thereafter. PID control algorithm has slow response time and the trajectory error of joint position is great.

However, due to the on-line adjustment of the PID parameters and the inherent time lag of the PAM control system, the joint has a relatively severe jitter phenomenon during the control process. To solve this problem, a low-pass filter is added to the control loop to smooth the output of the RBFNN-PID control algorithm, and the experimental curves can be obtained as shown in Fig. 10 and Fig. 11.

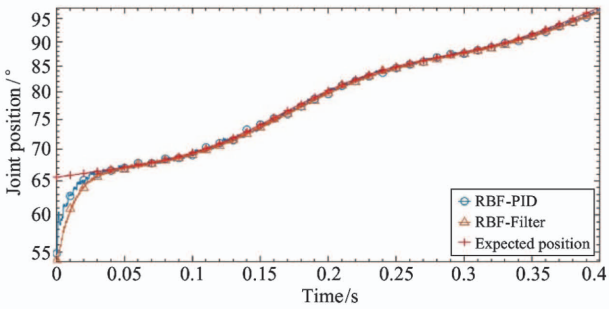

Fig. 10 Trajectory tracking curve 3

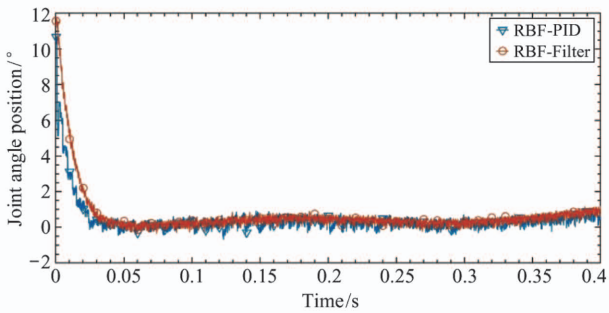

Fig. 11 Trajectory tracking error curve 3

Before the addition of the filter, the joint jitter reaches about 1 °, and after the addition of the filter, the joint jitter decreases to 0.5 °. It can be seen from Fig. 11 that the variation range of joint error decreases from 0.7 ° to 0.2 °.

4.3 Jumping experiment

In order to verify the bionic leg can realize jumping action under control, a jumping experiment is carried out. The experimental results are shown in Fig. 12. In order to achieve forward jump of the bionic leg, the initial posture of the bionic leg is adjusted as shown in Fig. 12(a). The center of mass of the bionic leg rises under the action of pneumatic muscle force,

and the toes gradually leave the ground, as shown in Fig. 12(b) and (c). When the speed of single leg reaches a certain level, the toes completely leave the ground, as shown in Fig. 12(d). When the bionic leg completely leave the ground, it also has a forward speed, as shown in Fig. 12(e) – (g). When the bionic leg reaches the highest point, it starts to retract the leg to achieve a more stable landing, as shown in Fig. 12(h).

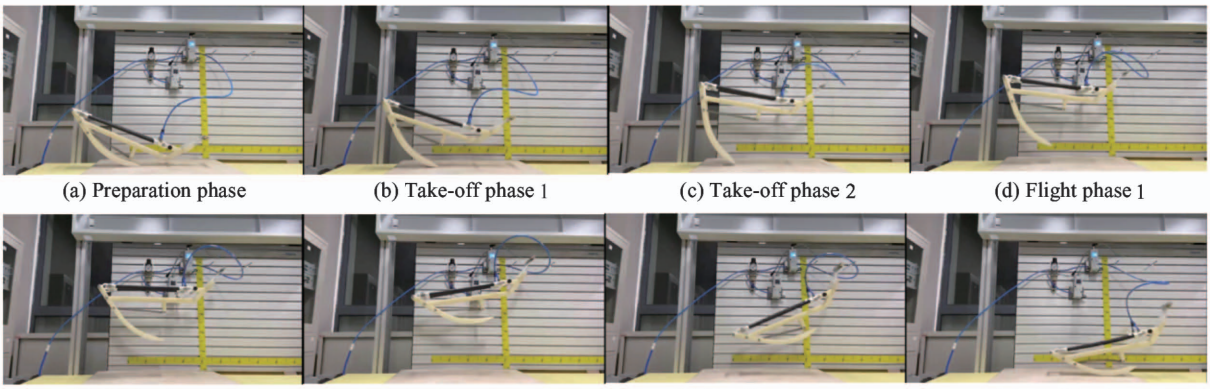

(a) Preparation phase (b) Take-off phase 1 (c) Take-off phase 2 (d) Flight phase 1

(e) Flight phase 2 (f) Landing phase 1 (g) Landing phase 2 (h) End of the jump

Fig. 12 Jump experiment

The jump process time of the bionic leg is about 0.4 s, the maximum height of jump movement is about 250 mm, and the forward jump distance is about 500 mm. In the experiment, it is found that the change of pneumatic artificial muscle force and the movement of the center of gravity of the bionic leg have a greater impact on the landing of the bionic leg, and it is difficult for the bionic leg to obtain a stable landing posture.

5 Conclusions

A bionic leg with single degree of freedom driven by one PAM is presented. Aiming at the nonlinearity and time lag of PAM, RBFNN is used to optimize the PID controller to realize high-precision position control of joint. Aiming at the problem that the intelligent control algorithm may cause joint jitter, a filter is added to the control loop to improve the control stability. Simulation and experimental results show that RBFNN-PID control algorithm has good control effect and dynamic performance than PID control algorithm. Jumping experiments show that the bionic leg can achieve the horizontal displacement of 500 mm and the vertical displacement of 150 mm.

Reference

[1] Wang G B, Chen D S, Chen K W, et al. The current research status and development strategy on biomimetic robot [J]. *Journal of Mechanical Engineering*, 2015, (13): 27-44 (In Chinese)

[2] Li Z, Gao J. Analysis of landing impact force of the one-legged robot vertical hopping[J]. *Journal of Harbin Institute of Technology*, 2017, 49(7): 27-32 (In Chinese)

[3] Jun Z, Guang M S, Yu Y L, et al. A bio-inspired jumping robot: modeling, simulation, design, and experimental results[J]. *Mechatronics: The Science of Intelligent Machines*, 2013, 8(8): 1123-1140

[4] Zhang D H, Zhao X G, Han J D. Active model-based control for pneumatic artificial muscle[J]. *IEEE Transactions on Industrial Electronics*, 2017, 64(2): 1686-1695

[5] Sui L, Zhao T, Zhang L X. Strategy for the position control of joint actuated by pneumatic muscles[J]. *Chinese Hydraulics and Pneumatics*, 2008, (6): 11-13 (In Chinese)

[6] Liu K, Ge Z S, Xu J Q, et al. Kinematic optimization of bionic shoulder driven by pneumatic muscle actuators based on particle swarm optimization[J]. *Transactions of Nanjing University of Aeronautics and Astronautics*, 2016, 33(3): 301-309

[7] Wang B R, Shen G Y, Jin Y L, et al. Sliding mode control of cascade pneumatic muscles of elbow joint based on disturbance observer[J]. *Acta Armamentarii*, 2017, 38(4): 793-801 (In Chinese)

[8] Shen W, Shen G L. Pneumatic artificial muscle discrete sliding mode displacement tracking control[J]. *Chinese Hydraulics and Pneumatics*, 2010, (9): 27-29 (In Chinese)

[9] Ba D X, Ahn K K, Tai N T. Adaptive integral-type neural sliding mode control for pneumatic muscle actuator [J]. *International Journal of Automation Technology*, 2014, 8(6):888-895

[10] Xie J, Tao G, Zhou H. Sliding mode tracking control of pneumatic muscle joint actuated by high-speed on-off solenoid valve[J]. *China Mechanical Engineering*, 2007, 18(5): 540-544 (In Chinese)

[11] Wang Y, Zhang Q, Xiao X H. Trajectory tracking control of the bionic joint actuated by pneumatic artificial muscle based on robust modeling[J]. *Robot*, 2016, 38(2):

248-256 (In Chinese)
[12] Thanh T U D C, Ahn K K. Nonlinear pid control to improve the control performance of 2 axes pneumatic artificial muscle manipulator using neural network[J]. *Mechatronics*, 2006, 16(9): 577-587
[13] Wang Y, Shi Z X, Wang J R, et al. Study of smooth and accurate position controls of pneumatic artificial muscle actuators for robotic arms[J]. *Advanced Materials Research*, 2011, 317-319: 799-806
[14] Jiang X Z, Huang X H, Xiong C H, et al. Position control of a rehabilitation robotic joint based on neuron proportion-integral and feedforward control[J]. *Journal of Computational and Nonlinear Dynamics*, 2012, 7(2): 1-6
[15] Wang J, Jiang X Z. Modeling of rehabilitation robot joint driven by pneumatic muscle and position control with fuzzy control algorithm[J]. *Machinery*, 2011, 49(3): 10-13 (In Chinese)
[16] Guo M, Tu X K, He J P, et al. Wearable upper-limb robot for rehabilitation based on fuzzy PI control[J]. *Journal of Huazhong University of Science and Technology (Nature Science Edition)*, 2015(z1): 355-358 (In Chinese)
[17] Wang B R, Zhang B, Shen G Y, et al. Modeling and fuzzy control of humanoid elbow driven by cascaded pneumatic muscles[J]. *Robot*, 2017, 39(4): 474-480 (In Chinese)
[18] Gao J, Ge W J. Research of fuzzy adaptive controller for single joint hopping robot[J]. *Computer Simulation*, 2013, 30(2): 331-335 (In Chinese)
[19] Nuchkrua T, Leephakpreeda T. Fuzzy self-tuning PID control of hydrogen-driven pneumatic artificial muscle actuator[J]. *Journal of Bionic Engineering*, 2013, 10(3): 329-340
[20] Zhu J M, Huang C Y, Lei J T, et al. Position/Stiffness control of antagonistic bionic joint driven by pneumatic muscles actuators[J]. *Journal of Mechanical Engineering*, 2017, 53(13): 64-74 (In Chinese)
[21] Chou C P, Hannaford B. Measurement and modeling of mckibben pneumatic artificial muscle[J]. *IEEE Transaction on Robotics and Automation*, 1996, 12(1): 90-102
[22] Zhang J H, Xu X L, Liu X, et al. Relative dynamic modeling of dual-arm coordination robot[J]. *Journal of Mechanical Engineering*, 2019, 55(3): 34-42 (In Chinese)

Su Hongsheng, born in 1996. He received his B. S. degree from Nanjing Institute of Technology in 2018. Now he is a postgraduate student in School of Mechatronic and Engineering Automation, Shanghai University. His research interest is bionic robot technology.